

**Fast quantum driving in two-level systems with interaction and nonlinear sweep**Fu-Quan Dou,<sup>1,\*</sup> Jie Liu,<sup>2,3,†</sup> and Li-Bin Fu<sup>3,4,‡</sup><sup>1</sup>*College of Physics and Electronic Engineering, Northwest Normal University, Lanzhou 730070, China*<sup>2</sup>*Laboratory of Computational Physics, Institute of Applied Physics and Computational Mathematics, Beijing 100088, China*<sup>3</sup>*HEDPS, CAPT, and CICIFSA MoE, Peking University, Beijing 100871, China*<sup>4</sup>*Graduate School, China Academy of Engineering Physics, Beijing 100193, China*

(Received 24 January 2018; published 1 August 2018)

We investigate high-fidelity fast quantum driving in a generalized nonlinear two-level system with both interparticle interaction and nonlinear energy sweep. We find that fast quantum dynamics depend on the interaction, energy sweep parameter, and energy sweep strength. We show that the driving protocol for a large energy sweep parameter reaches a given final high fidelity in a shorter time. The interparticle interaction can influence the quantum driving dynamics and can even break the quantum speed limit of the linear model. For the attractive interaction, the minimal time decreases monotonically as energy sweep strength increases, while it increases for the repulsive interaction. We also study a critical behavior and obtain analytical expressions of a critical interaction or a critical sweep strength, beyond which the target state cannot be achieved with high fidelity.

DOI: [10.1103/PhysRevA.98.022102](https://doi.org/10.1103/PhysRevA.98.022102)**I. INTRODUCTION**

The precise control of quantum systems is an important and challenging problem in many areas [1–4], ranging from quantum information [5,6], quantum optics [7], Bose-Einstein condensates (BECs), and nuclear magnetic resonance, to quite general atomic, molecular, and chemical physics [8,9]. Speed, fidelity, and robustness are three essential characteristics of quantum control schemes [10]. There is a fundamental limit which is set by quantum mechanics: this is the maximum speed, rooted in the Heisenberg time-energy uncertainty principle, at which a quantum system can evolve [11]. Quantum speed limits (QSLs) answer the fundamental question of how fast a quantum system can evolve and determine the theoretical upper bound on the speed of evolution of a quantum system [12–16]. Manipulation of the quantum system requires a control protocol not only to be implemented with the maximal speed, i.e., in the shortest possible time in order to minimize the role of decoherence [17,18], but also to assure high fidelity and robustness against variations in the field parameters. To this end, some optimal control techniques have been developed [19–21] and several different shortcuts to adiabaticity methods have been discussed [22,23]: quantum brachistochrone [24], fast-forward method [25], superadiabatic (or transitionless, counterdiabatic) quantum driving [26–28], and dressed state scheme [29].

However, most of the experimental explanations and associated theoretical discussions are limited to a linear two-level system [30,31]. In fact, the actual physics system is a nonlinear quantum system. Traditionally, there are two basic modifications of the original linear two-level system which differ by the basic type of the involved nonlinearity. In the first

case, the nonlinearity is accounted for by adding interaction terms to the basic linear equations describing the original linear two-level problem [32,33], which describes a BEC in a time-dependent two-state system in the mean-field approximation. In the second case, the energy bias is a nonlinearly sweeping external field which could be used to manipulate the system in a desired way [34,35]. The nonlinearity can significantly influence the quantum transition dynamics [32–36], especially in the ultracold Bose-Einstein condensate (BEC) system. The combined effect of particle interaction and nonlinear sweep on the Landau-Zener (LZ) transition has been studied and many interesting phenomena have been found [37]. For high-fidelity quantum driving, however, only very recently has this framework been extended so as to cope with the rich phenomenology and complexity of nonlinear quantum systems [38–41]. The high-fidelity superfast quantum driving have been achieved experimentally in a generalized LZ model with a nonlinear energy sweep [42]. The high-fidelity superfast quantum driving has also been investigated in a nonlinear two-level system with particle interaction for LZ, RC (Roland-Cerf), and CP (composite pulse) models [43]. However, the previous superfast quantum driving studies only consider either the interaction or nonlinear sweep [42,43]. These make it interesting to examine what happens if a superfast process is subject to both an interparticle interaction and a nonlinear energy sweep, as introduced above.

In this paper, we report our results of superfast quantum driving in a nonlinear two-level system with both interparticle interaction and nonlinear energy sweep. We show that the high-fidelity superfast quantum dynamics depend on the interparticle interaction, nonlinear energy sweep parameter, and energy sweep strength. In particular, we find a critical value of the attractive and repulsive interaction or the energy sweep strength, beyond which the minimal time becomes infinity, i.e., the high fidelity cannot be reached. Section II briefly introduces the two-level model. Section III investigates

\*doufq@nwnu.edu.cn

†liu\_jie@iapcm.ac.cn

‡lbfu@iapcm.ac.cn

the superfast quantum driving in the nonlinear model. The conclusions and possible experimental realization are given in Sec. IV.

## II. MODEL

The nonlinear two-level system is described by the dimensionless Schrödinger equation [33]

$$i \frac{\partial}{\partial t} \begin{pmatrix} a(t) \\ b(t) \end{pmatrix} = H(t) \begin{pmatrix} a(t) \\ b(t) \end{pmatrix}, \quad (1)$$

with the Hamiltonian given by

$$H(t) = [\Gamma(t) + c(|b(t)|^2 - |a(t)|^2)]\hat{\sigma}_z + \omega(t)\hat{\sigma}_x. \quad (2)$$

As usual,  $a(t)$  and  $b(t)$  are the probability amplitudes of diabatic state  $|0\rangle$  and  $|1\rangle$ . The total probability  $|a(t)|^2 + |b(t)|^2$  is conserved and set to be 1.  $\hat{\sigma}_x$  and  $\hat{\sigma}_z$  are Pauli matrices, and  $\Gamma(t)$  and  $\omega(t)$  are the energy bias and coupling strength between two diabatic levels, respectively. The parameter  $c$  denotes the particle interaction. In our model,  $c < 0$  represents the repulsive interaction, while  $c > 0$  characterizes the attractive interaction.

The above system has instantaneous adiabatic eigenstates  $|\psi_{g,e}(t)\rangle$ , where the subscripts  $g$  and  $e$  stand for the ground state and the excited state, respectively. We assume that the system is initially prepared in the adiabatic ground state  $|\psi_g(0)\rangle$  at time  $t = 0$ . The final state at time  $t = T$  is the state  $|\psi_{\text{fin}}\rangle$  after an evolution of duration  $T$ . For simplicity, we introduce the rescaled time  $\tau = t/T$ ,  $\tau \in [0, 1]$ . We consider a general model in which the coupling strength is constant and the energy bias is a nonlinear function of time [34,35,37,42],

$$\omega(\tau) = \omega(\text{const}), \quad \Gamma(\tau) = \text{sgn}(\tau - \frac{1}{2})\Gamma_0|2(\tau - \frac{1}{2})|^\beta, \quad (3)$$

where the parameter  $\Gamma_0$  is energy sweep strength, which stands for the energy sweep ranges from  $-\Gamma_0$  to  $\Gamma_0$ .  $\beta$  controls the nonlinearity of the energy sweep, called the power-law parameter or nonlinear energy sweep parameter. The model (3) has been used to investigate the quantum transition dynamics and the high-fidelity quantum driving [34,37,42]. Our aim is to employ the quantum control protocols (3) that drive the nonlinear system (2) from the starting state  $|\psi_{\text{ini}}\rangle = |\psi_g(0)\rangle$  to the final state  $|\psi_{\text{fin}}\rangle$  in the shortest possible time (i.e.,  $T$ ). Moreover, at the end of the evolution ( $\tau = 1$ ), the final state  $|\psi_{\text{fin}}\rangle$  is as close as possible to the adiabatic ground state  $|\psi_g(1)\rangle$ , realizing a high fidelity close to unity. Here the fidelity function  $F_{\text{fin}}$  is defined as follows:

$$F_{\text{fin}} = |\langle \psi_{\text{fin}} | \psi_g(T) \rangle|^2, \quad (4)$$

which can be used to characterize the protocol efficiency.

It is clear that for different time dependence  $\Gamma(\tau)$  and  $\omega(\tau)$ , the designed protocols may be accordingly different. For the case  $\beta = 1$ , the sweep is linear, corresponding to the LZ protocol, while the case  $\beta \rightarrow \infty$  stands for the CP protocol. Figure 1 shows the time dependence of  $\Gamma$  for different energy sweep parameters  $\beta$ .

When  $c = 0$ , three special cases, namely, the LZ model ( $\beta = 1$ ), the RC model, and the CP model ( $\beta \rightarrow \infty$ ), have been used to implement experimentally the high-fidelity fast

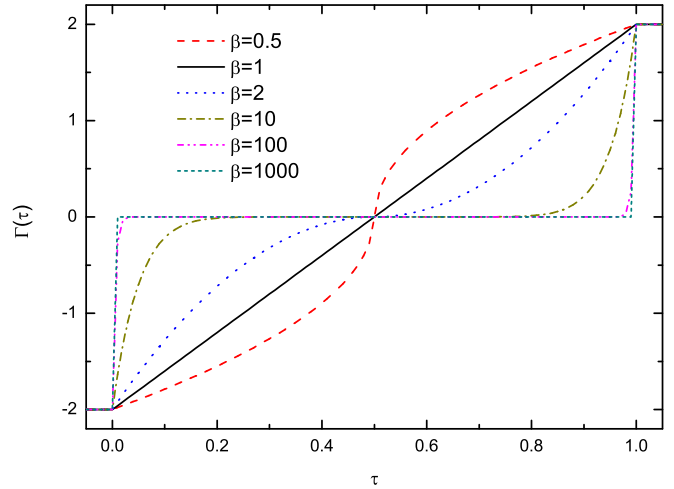


FIG. 1. The time dependence of  $\Gamma(\tau)$  for different energy sweep parameters  $\beta$  with  $\Gamma_0 = 2$ .

quantum driving for a two-level system comprising BEC in optical lattices [30]. It is pointed out that although the fact that the CP protocol realizes the quantum speed limit suggests that this time is optimal, a formal proof for this is still lacking [30]. Here the quantum speed limit time is given by [20,30]

$$T_{qsl} = \frac{\arccos |\langle \psi_{\text{fin}} | \psi_{\text{ini}} \rangle|}{\omega}. \quad (5)$$

Following the recipe of Ref. [30], high-fidelity quantum driving also has been experimentally implemented in a generalized two-level system with nonlinear sweep for  $\Gamma_0 = 2$  and it has been found that the minimal time of reaching the final state is shorter for the large sweep parameter  $\beta$  [42]. Furthermore, the superfast quantum driving has also been studied in the nonlinear two-level system ( $c \neq 0$ ) for the above three cases with  $\Gamma_0 = 2$  and it has been found that the interaction can influence the speed of quantum driving [43].

## III. NONLINEAR SUPERFAST QUANTUM DRIVING

We want to investigate the superfast quantum driving in the presence of both interparticle interaction and nonlinear energy sweep and consider how the interparticle interaction, the nonlinear energy sweep, and the energy sweep strength would affect the superfast quantum driving. With the emergence of two types nonlinearity, the Schrödinger equation (1) is no longer analytically solvable. We therefore exploit a fourth-fifth order Runge-Kutta algorithm to trace the quantum evolution numerically.

We examine the dynamics of the system (1) with (3) for various values  $c$  and  $\beta$ . In Fig. 2, the fidelity of the final state for  $\beta = 0.5, 1, 10, 100, 1000$  in different nonlinear interactions  $c/\omega = -4, -1, 0, 1, 1.7, 1.72$  is plotted as a function of the total duration  $T$  of the sweep. For comparison with the experimental result [30,42], we keep  $\omega = 0.5$  and  $\Gamma_0 = 2$  fixed. We find that the fidelity of the final state exhibits an oscillatory behavior and is strongly dependent on both the nonlinear interaction and the energy sweep parameter. It is evident that the maximal amplitude of the oscillatory can reach the value 1 for some parameters, while for the other

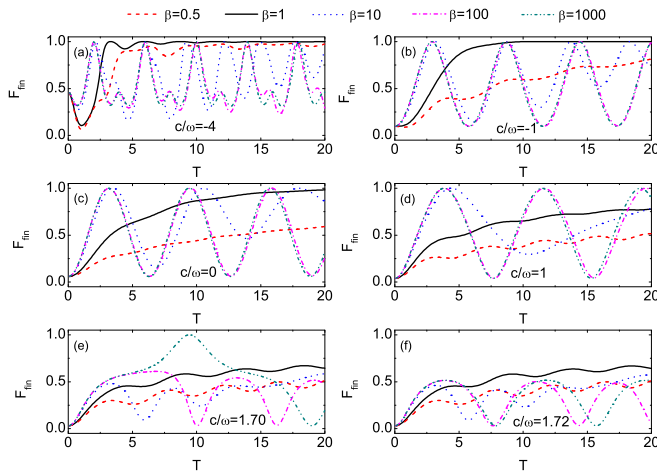


FIG. 2. The fidelity of the final state as a function of the duration in different energy sweep parameters and nonlinear interactions.

parameters, the value 1 cannot be reached. For different  $\beta$  and  $c$ , the dynamics of the designed protocol is accordingly different. When  $\beta = 1$ , the oscillatory behavior is a standard Rabi oscillation. The value of  $\beta$  and  $c$  can affect the period of the oscillation.

More interestingly, the sweeps with larger value  $\beta$  reach a given final fidelity in a shorter time. Fixing a threshold value at  $F_{\text{fin}} = 0.9$ , the required sweep duration  $T_{0.9}$  depends on  $\beta$  and  $c$ , as shown in Fig. 3. For the same interaction value, similar to the result of Refs. [30,42], the minimal time arriving to the desired final state with high fidelity decreases as the energy sweep parameter increases. For large energy

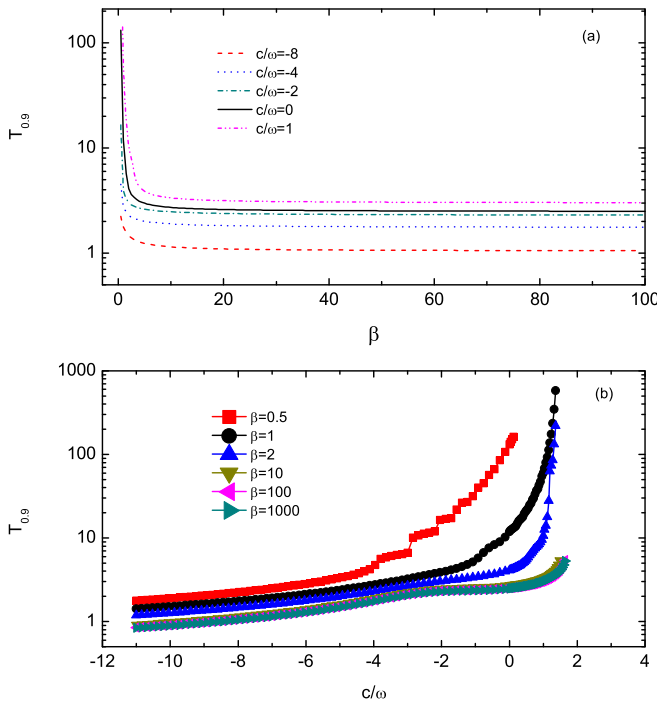


FIG. 3. The minimal time to achieve fidelity  $F_{\text{fin}} = 0.9$  as a function of (a) the energy sweep parameter  $\beta$  for different nonlinear interaction and (b) the interaction  $c$  for different energy sweep in a semilogarithmic scale.

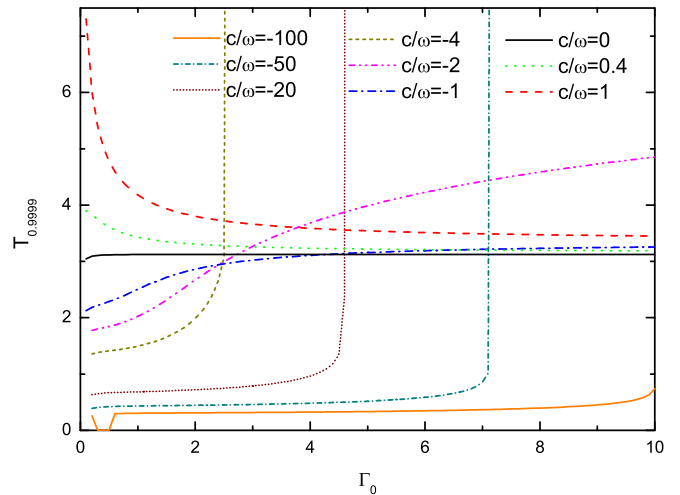


FIG. 4. The minimal time to reach the fidelity  $F_{\text{fin}} = 0.9999$  as a function of the parameter  $\Gamma_0$  for different nonlinear interaction with  $\beta = 1000$ .

sweep parameter value  $\beta$ ,  $T_{0.9}$  approaches the minimum time [Fig. 3(a)]. However, for the same value of energy sweep parameter, the minimal time arriving to the desired final state gradually increases with the nonlinear interaction from repulsion to attraction and tends to two different limit values for strong enough attractive and repulsive interaction. Without interaction (i.e.,  $c = 0$ ), for large enough  $\beta$ , the minimal time  $T_{0.9}$  approaches the quantum speed limit for the parameters of a linear two-level system. For the strong enough attractive interaction, the minimal time to reach  $F_{\text{fin}} = 0.9$  diverges (i.e., cannot realize the high fidelity), while it reach a minimal value even far less than the quantum speed limit time of the linear system for strong repulsive interaction [Fig. 3(b)]. This implies that the superfast quantum control with high fidelity will no longer be achieved for the large enough attractive interaction strength and the quantum speed limit of the linear model breaks in strong enough repulsive interaction.

Hitherto, our studies show that the minimal time arriving to the desired final state with high fidelity is strongly dependent on the interaction and energy sweep parameter. The superfast quantum driving can also optimize the excitation with respect to the sweep strength parameters  $\Gamma_0$ . To test the sensitivity of the different protocol to a variation in the control parameters, we vary  $\Gamma_0$  and calculate the duration  $T_{0.9999}$  for  $\beta = 1000$ . In this case, the protocol approaches the form of the CP protocol. In Fig. 4, we plot the minimal time  $T_{0.9999}$  as a function of the parameters  $\Gamma_0$  for different nonlinear interactions. We find that the minimal time to reach  $F_{\text{fin}} = 0.9999$  is also dependent on the parameter  $\Gamma_0$ . For the attraction interaction, the minimal time  $T_{0.9999}$  decreases monotonically with  $\Gamma_0$ , and can arrive at the value of quantum speed limit time of the linear system for the large enough  $\Gamma_0$ . However, it increases with  $\Gamma_0$  for the repulsion interaction, and the value of  $T_{0.9999}$  is divergent for some special  $\Gamma_0$ . The quantum speed limit of a linear two-level system is broken for a wide range of parameters  $c$ ,  $\Gamma_0$  and even  $T_{0.9999}$  is far less than the quantum speed limit time for the strong enough repulsive interaction. This is due to the existence of Josephson oscillation at this parameter

region and the interaction can influence the oscillation period. When the interaction is large enough, for the special  $\Gamma_0$ , the  $T_{0,9999}$  is divergent and the superfast quantum driving cannot be achieved. At the moment, the system becomes self-trapped. The high-fidelity quantum driving will no longer be achieved and the critical behavior appears.

To further investigate the dependence of the minimal time on nonlinear interaction  $c$ , energy sweep parameter  $\beta$ , and the parameter  $\Gamma_0$ , and to understand the critical behavior, we will focus on the parameter regime with the large energy sweep parameter value  $\beta$ . From the above analysis, we see that the system exists the Josephson oscillation and the self-trapped phenomena for some parameters. For instance, for the weak attractive interaction, Josephson oscillation will be observed. When the interaction is large enough and over a critical value, the system becomes self-trapped. As a result, the superfast quantum control with high fidelity will no longer be achieved for the parameter regime. When the self-trapped case occurs, the energy of the system described by a classical Hamiltonian,  $H_{\text{eff}}(c, \omega) = -c(1 - 2|a|^2)^2/2 - \omega\sqrt{1 - (1 - 2|a|^2)^2}$ , is smaller than  $-\omega$  for the attractive interaction ( $c > 0$ ), while  $H_{\text{eff}}(c, \omega)$  is larger than  $\omega$  for the repulsive interaction ( $c < 0$ ) [36,44]. Therefore, we can obtain the general criterion for the occurrence of the critical behavior, i.e., the classical Hamiltonian of the system  $H_{\text{eff}}(c, \omega) < -\omega$  ( $c > 0$ ) or  $H_{\text{eff}}(c, \omega) > \omega$  ( $c < 0$ ). Then the critical criteria are expressed as

$$\left(\frac{c}{\omega}\right)_{cra} > \frac{2[1 - \sqrt{1 - (1 - 2|a_i|^2)^2}]}{(1 - 2|a_i|^2)^2}, \quad c > 0, \quad (6)$$

$$\left(\frac{c}{\omega}\right)_{crp} < -\frac{2[1 + \sqrt{1 - (1 - 2|a_i|^2)^2}]}{(1 - 2|a_i|^2)^2}, \quad c < 0, \quad (7)$$

where  $|a_i|^2$  is the corresponding population of the initial state. When the parameters satisfy (6) and (7), the superfast quantum control with high fidelity will no longer be achieved. According to Eqs. (6) and (7), we can also obtain the critical values for high-fidelity and non-high-fidelity quantum control. For example,  $(c/\omega)_{cra} = 1.7044$  for  $\Gamma_0 = 2$  [see, also, Fig. 2(a)]. Different values of  $\Gamma_0$  correspond to different critical values of  $c/\omega_{cra}$ . Similarly, we can also obtain the critical values of  $\Gamma_0$  in different repulsive interaction  $c$ . For instance,  $\Gamma_0 = 2.59808$  for  $c/\omega = -4$ . In Fig. 5, we plot the parameter regime of  $c/\omega, \Gamma_0$  for achieving high-fidelity quantum control. The yellow zone represents high fidelity that can be achieved in the parameter regime, whereas the shadow zone corresponds to the parameter regime which cannot achieve the high-fidelity quantum driving. The red point corresponds to the parameter value  $(\Gamma_0, c/\omega) = (2.59808, -4)$ . It is clear that for attractive interactions, when  $c/\omega < c/\omega_{cra}$ , the high-fidelity quantum driving can be achieved; when  $c/\omega$  exceeds the value of  $c/\omega_{cra}$ , the high-fidelity quantum driving cannot be achieved. For repulsive interactions, when  $\Gamma_0 < 2.59808$ , the high-fidelity quantum driving can be achieved for all the repulsive interactions. However, when  $\Gamma_0 > 2.59808$ , the high-fidelity quantum driving will no longer be achieved at some repulsive interaction regimes.

Now, in order to recover the time-optimal trajectory on a geodesic, we impose geometrical considerations for the above control protocols. Such time-optimal dynamics occurs along

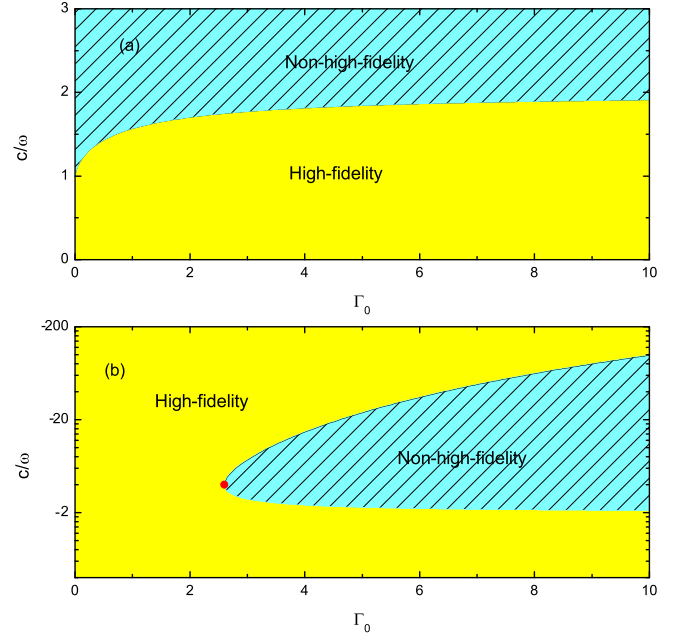


FIG. 5. Phase diagram as functions of the parameter  $\Gamma_0$  and interaction  $c/\omega$ . (a)  $c > 0$ ; (b)  $c < 0$ . The red point corresponds to the parameter value  $(\Gamma_0, c/\omega) = (2.59808, -4)$ .

a geodesic on the Bloch sphere connecting the initial and the target state. On the Bloch sphere, the quantum driving protocols for the different parameters have a very simple description [40]. The initial and final states correspond to points on the Bloch sphere lying symmetrically with respect to the near north pole and south pole, and each driving protocol corresponds to a path from the initial state to final state. Figure 6 shows the different paths on the Bloch sphere for the different interactions and sweep parameters for  $\beta = 1$  (blue dashed line),  $\beta = 2$  (red dash-dotted line), and  $\beta = 1000$  (olive solid line): (a)  $c/\omega = -2$ , where the green line describes  $\beta = 0.5$ , (b)  $c/\omega = 0$ , and (c)  $c/\omega = 1$ . The blue and red stars represent the initial and the target states, respectively. It is obvious that the path is shorter for large  $\beta$ , indicating that the speed of quantum driving is faster (i.e., the minimal time to arrive at the final state is shorter). For small  $\beta$ , for example,  $\beta = 0.5$  [Fig. 6(a)] and  $\beta = 1$  [Figs. 6(b) and 6(c)], to achieve high

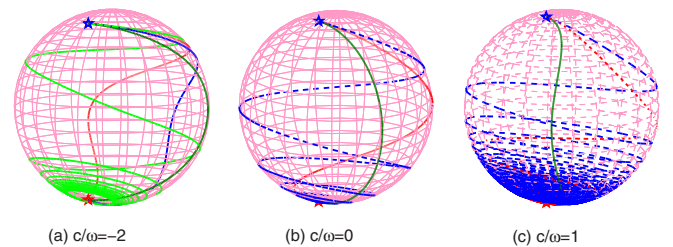


FIG. 6. Bloch sphere representation of different paths for the different interactions and sweep parameters for  $\beta = 1$  (blue dashed line),  $\beta = 2$  (red dash-dotted line), and  $\beta = 1000$  (olive solid line): (a)  $c/\omega = -2$ , where the green line describes  $\beta = 0.5$ ; (b)  $c/\omega = 0$ ; and (c)  $c/\omega = 1$ . The blue and red stars represent the initial and the target states, respectively. The value of parameter  $\Gamma_0 = 2$ .



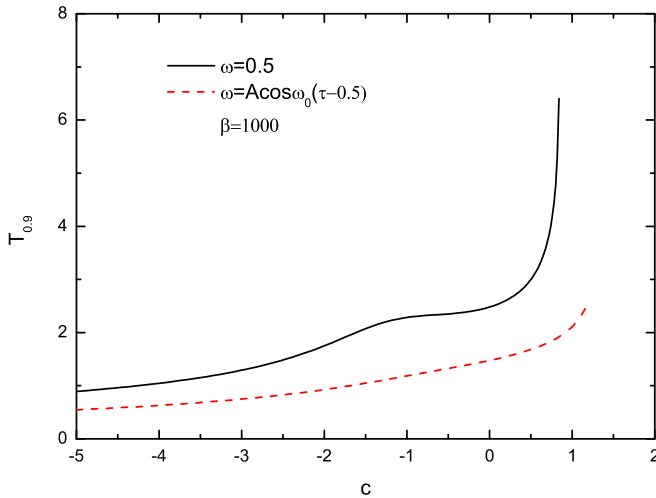


FIG. 7. The minimal time to achieve fidelity  $F_{\text{fin}} = 0.9$  as a function of the interactions  $c$  for  $\omega = A \cos \omega_0(\tau - 0.5)$  and  $\omega = 0.5$  with  $\beta = 1000$ ,  $A = 1$ , and  $\omega_0 = 2\pi/3$ .

fidelity, the path is longer and is winding on the Bloch sphere, especially near the desired final state.

#### IV. DISCUSSIONS AND CONCLUSIONS

To compare the previous experimental and theoretical results, we focus our attention on the control of Eq. (3) [i.e.,  $\Gamma(\tau)$  is a time-dependent function, while  $\omega(\tau)$  is a fixed constant], which includes a series of a model, such as the famous LZ and CP models. In general, one can extend the control protocol to more general situations. It is very interesting and valuable to consider the control of both  $\omega(\tau)$  and  $\Gamma(\tau)$  in a more complicated form. In particular, the coupling strength  $\omega(\tau)$  can also be a time-dependent function. For an example, we discuss the high-fidelity fast quantum driving by taking  $\omega = A \cos \omega_0(\tau - 0.5)$  [45]. In Fig. 7, we display the  $T_{0.9}$  as a function of  $c$  for both  $\omega = A \cos \omega_0(\tau - 0.5)$  and  $\omega = 0.5$  (constant) with  $A = 1$ ,  $\omega_0 = 2\pi/3$ , and  $\beta = 1000$ . The comparison shows that there is a quantitative influence of them on the control results. We also find that the time-dependent control scheme can achieve the same goal of time-independent control protocol by optimizing control field parameters.

In conclusion, we have investigated the high-fidelity fast quantum driving in a nonlinear two-level system and explored the combined effect of atomic interactions and nonlinear sweep on high-fidelity superfaster quantum driving. An important result of the present work is that for the same interaction value, the minimal time for reaching the target state is shorter for larger sweep parameter, and the quantum speed limit is also reached by the generalized nonlinear protocol in weak attractive interaction or without attractive interaction for large sweep strength. We have found that repulsive interaction between particles is inclined to decrease the minimal time for reaching the target state, even far less than the quantum speed limit time of the linear system for some certain parameter region of the energy sweep strength, resulting in a breakdown of the quantum speed limit of the linear model. However, no matter what the interaction is, there always exists a critical value of the interaction strength beyond which the superfaster quantum driving cannot be achieved with a high fidelity. The critical interaction and sweep strength values have been obtained analytically. The fast quantum driving in a nonlinear two-level system can be realized experimentally using BECs between Bloch bands in an accelerated optical lattice. The mathematical model for this system can be described by Eq. (1), where the time dependence of  $\Gamma(\tau)$ ,  $\omega$ , and  $c$  can be controlled through the quasimomentum, the depth of the optical lattice, and the atomic density or Feshbach resonance, respectively [42,46–48]. The system is initially prepared in the lowest-energy band of the lattice with  $q = 0$  (corresponding to  $|\psi_{\text{ini}}\rangle$ ), and the target is to reach  $|\psi_{\text{fin}}\rangle$  after an evolution of duration  $T$ . It is noted that the choice of  $\omega(\tau)$  and  $\Gamma(\tau)$  may be taken in an arbitrary optimal form principally. It is a very interesting and valuable topic to study the high-fidelity quantum driving when the coupling strength and the energy bias are more complicated control strategies.

#### ACKNOWLEDGMENTS

We thank H. Cao, H. D. Liu, S. C. Li, and W. Y. Wang for helpful discussions. The work is supported by the National Basic Research Program of China (973 Program) (Grants No. 2013CBA01502 and No. 2013CB834100), the National Natural Science Foundation of China (Grants No. 11665020, No. 11547046, No. 11725417, No. 11475027, and No. 11575027), the Natural Science Foundation of Gansu Province, China (Grant No. 1606RJZA081), and the Scientific Research Foundation of NWNNU (Grant No. NWNNU-LKQN-16-3).

- 
- [1] C. Brif, R. Chakrabarti, and H. Rabitz, *New J. Phys.* **12**, 075008 (2010).
  - [2] P. Král, I. Thanopoulos, and M. Shapiro, *Rev. Mod. Phys.* **79**, 53 (2007).
  - [3] V. V. Flambaum and M. G. Kozlov, *Phys. Rev. Lett.* **99**, 150801 (2007).
  - [4] T. W. Hänsch, *Rev. Mod. Phys.* **78**, 1297 (2006); H. Sabbah, L. Biennier, I. R. Sims, Y. Georgievskii, S. J. Klippenstein, and I. W. M. Smith, *Science* **317**, 102 (2007).
  - [5] M. Nielsen and I. Chuang, *Quantum Computation and Quantum Information* (Cambridge University Press, Cambridge, 2000).
  - [6] T. D. Ladd, F. Jelezko, R. Laflamme, Y. Nakamura, C. Monroe, and J. L. O'Brien, *Nature (London)* **464**, 45 (2010).
  - [7] M. Fleischhauer, A. Imamoglu, and J. Marangos, *Rev. Mod. Phys.* **77**, 633 (2005).
  - [8] S. A. Rice and M. Zhao, *Optical Control of Molecular Dynamics* (Wiley, New York, 2000).
  - [9] R. A. Bartels, T. C. Weinacht, N. Wagner, M. Baertschy, C. H. Greene, M. M. Murnane, and H. C. Kapteyn, *Phys. Rev. Lett.* **88**, 013903 (2001); C. Sá de Melo, *Phys. Today* **61**, 45 (2008).
  - [10] F. Q. Dou, H. Cao, J. Liu, and L. B. Fu, *Phys. Rev. A* **93**, 043419 (2016); D. Daems, A. Ruschhaupt, D.

- Sugny, and S. Guérin, *Phys. Rev. Lett.* **111**, 050404 (2013).
- [11] K. Bhattacharyya, *J. Phys. A: Math. Gen.* **16**, 2993 (1983).
- [12] M. M. Taddei, B. M. Escher, L. Davidovich, and R. L. de Matos Filho, *Phys. Rev. Lett.* **110**, 050402 (2013); A. Emmanouilidou, X. G. Zhao, P. Ao, and Q. Niu, *ibid.* **85**, 1626 (2000).
- [13] A. del Campo, I. L. Egusquiza, M. B. Plenio, and S. F. Huelga, *Phys. Rev. Lett.* **110**, 050403 (2013); S. Deffner and E. Lutz, *ibid.* **111**, 010402 (2013).
- [14] G. C. Hegerfeldt, *Phys. Rev. Lett.* **111**, 260501 (2013); *Phys. Rev. A* **90**, 032110 (2014).
- [15] I. Marvian and D. A. Lidar, *Phys. Rev. Lett.* **115**, 210402 (2015); D. V. Villamizar and E. I. Duzzioni, *Phys. Rev. A* **92**, 042106 (2015).
- [16] I. Marvian, R. W. Spekkens, and P. Zanardi, *Phys. Rev. A* **93**, 052331 (2016); D. P. Pires, M. Cianciaruso, L. C. Céleri, G. Adesso, and D. O. Soares-Pinto, *Phys. Rev. X* **6**, 021031 (2016).
- [17] M. Schlosshauer, *Rev. Mod. Phys.* **76**, 1267 (2005).
- [18] L. C. L. Hollenberg, *Nat. Phys.* **8**, 113 (2012).
- [19] S. J. Glaser, U. Boscain, T. Calarco, C. P. Koch, W. Köckenberger, R. Kosloff, I. Kuprov, B. Luy, S. Schirmer, T. Schulte-Herbrüggen, D. Sugny, and F. K. Wilhelm, *Eur. Phys. J. D* **69**, 279 (2015).
- [20] T. Caneva, M. Murphy, T. Calarco, R. Fazio, S. Montangero, V. Giovannetti, and G. E. Santoro, *Phys. Rev. Lett.* **103**, 240501 (2009).
- [21] S. Lloyd and S. Montangero, *Phys. Rev. Lett.* **113**, 010502 (2014).
- [22] X. Chen, A. Ruschhaupt, S. Schmidt, A. del Campo, D. Guéry-Odelin, and J. G. Muga, *Phys. Rev. Lett.* **104**, 063002 (2010); S. Ibáñez, X. Chen, E. Torrontegui, J. G. Muga, and A. Ruschhaupt, *ibid.* **109**, 100403 (2012).
- [23] E. Torrontegui, S. S. Ibáñez, S. Martínez-Garaot, M. Modugno, A. del Campo, D. Guéry-Odelin, A. Ruschhaupt, X. Chen, and J. G. Muga, *Adv. At. Mol. Opt. Phys.* **62**, 117 (2013).
- [24] A. Carlini, A. Hosoya, T. Koike, and Y. Okudaira, *Phys. Rev. Lett.* **96**, 060503 (2006).
- [25] S. Masuda and K. Nakamura, *Phys. Rev. A* **84**, 043434 (2011).
- [26] M. Demiralp and S. A. Rice, *J. Phys. Chem. A* **107**, 9937 (2003); *J. Phys. Chem. B* **109**, 6838 (2005).
- [27] M. V. Berry, *J. Phys. A: Math. Theor.* **42**, 365303 (2009); R. Lim and M. V. Berry, *ibid.* **24**, 3255 (1991).
- [28] F. Q. Dou, J. Liu, and L. B. Fu, *Europhys. Lett.* **116**, 60014 (2016).
- [29] A. Baksic, H. Ribeiro, and A. A. Clerk, *Phys. Rev. Lett.* **116**, 230503 (2016).
- [30] M. G. Bason, M. Viteau, N. Malossi, P. Huillery, E. Arimondo, D. Ciampini, R. Fazio, V. Giovannetti, R. Mannella, and O. Morsch, *Nat. Phys.* **8**, 147 (2012).
- [31] J. Zhang, J. H. Shim, I. Niemeyer, T. Taniguchi, T. Teraji, H. Abe, S. Onoda, T. Yamamoto, T. Ohshima, J. Isoya, and D. Suter, *Phys. Rev. Lett.* **110**, 240501 (2013).
- [32] J. Liu, B. Wu, and Q. Niu, *Phys. Rev. Lett.* **90**, 170404 (2003); J. Liu and L. B. Fu, *Phys. Rev. A* **81**, 052112 (2010).
- [33] B. Wu and Q. Niu, *Phys. Rev. A* **61**, 023402 (2000); B. Wu and J. Liu, *Phys. Rev. Lett.* **96**, 020405 (2006); J. Liu, L. B. Fu, B. Y. Ou, S. G. Chen, D. I. Choi, B. Wu, and Q. Niu, *Phys. Rev. A* **66**, 023404 (2002).
- [34] D. A. Garanin and R. Schilling, *Phys. Rev. B* **66**, 174438 (2002); D. A. Garanin, *ibid.* **68**, 014414 (2003); J. Liu and L. B. Fu, *Phys. Lett. A* **370**, 17 (2007).
- [35] N. V. Vitanov and K. A. Suominen, *Phys. Rev. A* **59**, 4580 (1999); B. M. Garraway and N. V. Vitanov, *ibid.* **55**, 4418 (1997).
- [36] F. Trimborn, D. Witthaut, V. Kegel, and H. J. Korsch, *New J. Phys.* **12**, 053010 (2010).
- [37] F. Q. Dou, S. C. Li, and H. Cao, *Phys. Lett. A* **376**, 51 (2011).
- [38] P. Doria, T. Calarco, and S. Montangero, *Phys. Rev. Lett.* **106**, 190501 (2011).
- [39] S. Campbell, G. De Chiara, M. Paternostro, G. M. Palma, and R. Fazio, *Phys. Rev. Lett.* **114**, 177206 (2015).
- [40] I. Brouzos, A. I. Streltsov, A. Negretti, R. S. Said, T. Caneva, S. Montangero, and T. Calarco, *Phys. Rev. A* **92**, 062110 (2015).
- [41] X. Chen, Y. Ban, and G. C. Hegerfeldt, *Phys. Rev. A* **94**, 023624 (2016); S. Deffner and S. Campbell, *J. Phys. A: Math. Theor.* **50**, 453001 (2017).
- [42] N. Malossi, M. G. Bason, M. Viteau, E. Arimondo, R. Mannella, O. Morsch, and D. Ciampini, *Phys. Rev. A* **87**, 012116 (2013).
- [43] F. Q. Dou, L. B. Fu, and J. Liu, *Phys. Rev. A* **89**, 012123 (2014).
- [44] L. B. Fu and J. Liu, *Phys. Rev. A* **74**, 063614 (2006).
- [45] X. Miao, E. Wertz, M. G. Cohen, and H. Metcalf, *Phys. Rev. A* **75**, 011402 (2007); T. Lu, X. Miao, and H. Metcalf, *ibid.* **75**, 063422 (2007); T. Lu, *ibid.* **84**, 033411 (2011); D. M. Tong, K. Singh, L. C. Kwek, and C. H. Oh, *Phys. Rev. Lett.* **98**, 150402 (2007).
- [46] Y. A. Chen, S. D. Huber, S. Trotzky, I. Bloch, and E. Altman, *Nat. Phys.* **7**, 61 (2010).
- [47] M. Jona-Lasinio, O. Morsch, M. Cristiani, N. Malossi, J. H. Müller, E. Courtade, M. Anderlini, and E. Arimondo, *Phys. Rev. Lett.* **91**, 230406 (2003).
- [48] C. Chin, R. Grimm, P. Julienne, and E. Tiesinga, *Rev. Mod. Phys.* **82**, 1225 (2010).